IEEE Access
Multidisciplinary | Rapid Review | Open Access Journal

SPECIAL SECTION ON WIRELESS BODY AREA NETWORKS

Received June 3, 2019, accepted June 28, 2019, date of publication July 11, 2019, date of current version August 30, 2019.

Digital Object Identifier 10.1109/ACCESS.2019.2928055

Self-Sustainable Smart Ring for Long-Term Monitoring of Blood Oxygenation

MICHELE MAGNO[1], (Senior Member, IEEE), GIOVANNI A. SALVATORE[1,2], PETAR JOKIC[1], (Member, IEEE), AND LUCA BENINI[1], (Fellow, IEEE)

[1]Department of Information Technology and Electrical Engineering, ETH Zürich, 8092 Zürich, Switzerland
[2]ABB Research Centre, 5405 Baden, Switzerland

Corresponding author: Michele Magno (michele.magno@iis.ee.ethz.ch)

This work was supported in part by the Swiss National Science Foundation Projects MicroLearn: Micropower Deep Learning under Grant 162524, and in part by the Transient Computing Systems under Grant 157048.

ABSTRACT Medical devices measure vital parameters such as pulse, respiration rate, and blood oxygenation, over periods of days or weeks in a continuous manner. Traditional systems only support such requirements in stationary applications where a constant power supply is available. Trends toward remote healthcare and telemedicine require wearable devices, able to provide similar functionalities in wireless mode. Miniaturized and thin form factors, desirable in wearable applications, set stringent constraints on the available power, and consequently on the accuracy and lifetime. Energy harvesting combined with low-power design and energy efficient processing can significantly extend the lifetime of wearable devices. This paper presents a wearable pulse oximeter assembled in a 3D ring-like geometry that achieves self-sustainability by exploiting efficient power management, solar energy harvesting, and ultra-low power processing in a multi-core microcontroller. The design strategy of combining onboard processing to monitor blood oxygenation and the transmission of only relevant information via a Bluetooth low-energy (BLE) interface, significantly reduces the overall energy consumption. Experimental results on the designed and developed prototype demonstrate that measuring the blood oxygenation once every minute with a sampling rate of 100 samples/s achieve accurate results at the daily energy consumption of 28 J including hourly BLE transmissions. The low-power design allows the system to be self-sustainable with just 64 min of sunlight per day or 12 hrs. of indoor home light.

INDEX TERMS Wearable devices, energy harvesting, smart sensing, low power design, energy efficiency, self-sustaining.

I. INTRODUCTION

Advances in low power processors, wireless communication, energy harvesting, and sensors network are driving the pace of innovation in wearable devices. The number of commercial devices targeting wearable applications has increased by more than 25% from 2015 to 2016. Similar growth is forecasted for the next five years [1]. Due to the interest of companies developing wearable consumer electronics, wireless sensor devices attached in different ways to the human body have become successful products in the wellness, fashion and sports domains, with many applications interfaced directly *via* smartphones [2]–[10] Additionally, there has been a significant increase in interest in monitoring human health during daily activities [7], [8]. Wearable medical devices aimed at reducing hospitalization and, consequently, the costs of the health care system [9], [10]. Wearable devices are designed to regularly check the status of the patients, enable continuous monitoring in a noninvasive and comfortable manner [7] and alert users and medical professionals of abnormalities. Many chronic diseases, such as Chronic Obstructive Pulmonary Disease (COPD) [11], require the continuous monitoring of medical parameters such as heart rate (HR), respiratory rate (RR), blood oxygen saturation (SpO_2) [12]–[16]. Commercial products like Nonin Elite 3240 [5] iHealth PO3 [6] can acquire the heart rate, respiratory rate and oxygenation level with high accuracy and transfer these data to a remote host (phone or PC). Although these devices allow home-measurement, both provide only an on-demand solution, and the user has to decide when to use them.

Systems which can perform long-term and continuous monitoring are facing one major problem, namely the limited available energy in their batteries [14], [15]. To extend the lifetime of the device, and in that sense, maximize the

The associate editor coordinating the review of this manuscript and approving it for publication was Giancarlo Fortino.

possible monitoring time, the entire design (hardware and software) has to be optimized. On the one hand, the power consumption can be reduced by optimizing the data acquisition and processing (*i.e.,* duty-cycling, sleep-wake up, reducing radio activities, *etc.* [17]–[20]). Energy can be harvested from the environment or the body to constantly charge batteries and therefore compensate for the power being consumed [19], [21]. Increasing the battery capacity would be the simplest strategy, but it is, in most cases, impossible to implement due to size constraints. As these technologies are required to operate on the human body for long periods (i.e., days, or weeks), achieving self-sustaining systems by harvesting energy (EH) from environmental sources, movement or heat is particularly attractive [22], [23]. The most promising sources of energy for harvesting on and near the body include thermal, vibration, light and radio frequency (RF) [22], [23]. They can continuously provide average power in the range of μW when deployed on the human body. However, sunlight remains the EH source which can provide the highest energy density ($>100\mu$W/cm^2 in indoor conditions) [23].

The monitoring of blood oxygenation provides relevant information on the cardiovascular and respiratory system, and it is routinely performed in primary care during hospitalization [24]. The finger is a preferred and convenient region of the body for assessing SpO_2 [25]. There are several recent works in literature that are proposing the monitoring of blood oxygen with wireless wearable devices [26]–[31]. Authors in [26] presented an interesting recent review of the wearable sensor device for oxygenation saturation for infants. The review confirmed that previous approaches mainly send the data out to the acquisition device via the wireless interface, instead of processing them on board. In [27] and [28] the authors present two pulse measurement systems that are battery-less. However, as the systems need to receive power from Near Field Communication (NFC), they are able to work only in combination with a smartphone. The battery-less feature is interesting, but due to the limited resources of the NFC sensor, the wearable sensors have no capability of acquiring and processing data autonomously, so the long-term monitoring of the oxygenation is not possible. For this reason, those approaches are considered on-demand measurements more than smart long-term devices. On the other hand, battery-operated wireless wearable devices can acquire and send data to remote hosts. In [29] a microcontroller-based wireless wearable device is presented. The device has a near-infrared portable tissue oximeter with the goal of oxygenation monitoring. The node is capable of long term monitoring; however, the raw data are sent via wireless interface consuming around 20mA for the transmission. The same approach is used by authors in [30], where the authors proposed a wearable ear-worn device that transmits all the data to a smartphone via Bluetooth 4.0. Considering this, it is not surprising that the lifetime is only 10h with an 80mAh battery. Finally, in [30] the authors are presenting a wearable wireless device that has a Bluetooth interface and uses two sensors: an oximeter and an accelerometer to correct the artifacts due to the movement. The authors have shown the importance of this correction when the user is moving. However, also, in this case, all the data are streamed out to process the data with a smartphone or the PC. Also, commercial devices are available on the market to monitor the blood oxygenation level. Most of them are oximetry-based and look like a smart wristband worn on the wrist [5], [6]. In contrast to the previous academic works, the marked products exploit onboard processing to have an energy efficient device that can last a few days. Despite the previously presented works, this paper presents a ring-like, miniaturized, and low power system for the continuous monitoring of blood oxygenation. The smart ring includes an optimized energy harvesting circuit to recharge the battery and supply the device. Additionally, the smart ring can exploit solar energy harvesting using a thin, flexible solar panel [32] mounted on the 3D case of the ring. Onboard processing allows it to perform accurate blood oxygenation monitoring and to improve energy efficiency, transmitting only relevant data instead of the raw data. Due to the hardware-software co-design, it is possible to make the smart ring self-sustainable with just 64 minutes of sunlight exposure per day or 8h of indoor light.

TABLE 1. Comparison with other works.

Device	On-Demand / Plug and Forget	Energy Harv.	Onboard Process.	Lifetime [Days]
Noin Elite 3240 [5]	Y/N	N	Acquistion/ Analisys	2
iHelath PO3 [6]	Y/No	N	Acquistion/	5-10
			Analisys	
[27]	Y/N	Y	N	∞
[29]	Yes/No	N	Acquisition	2-4
[30]	Yes/No	N	Acquisition	1
This Work	**Yes/Yes**	**YES**	Acquisition /Analisys	∞

This paper focuses on the hardware and software co-design of a self-sustaining and energy efficient smart ring that includes a pulse oximeter to monitor blood oxygenation continuously and perpetually. The papers exploit the combination of energy harvesting and energy efficient onboard processing with the goal to have a neutral energy ring even using a small and flexible solar panel that works in indoor light condition. Moreover, the paper evaluates the energy efficiency of the onboard processing over the wireless transmission in the target application. Experimental results show the benefits of the proposed approach, the functionality, and the self-sustainability. To the best of our knowledge, this is the first ring-like pulse oximeter that achieves self-suitability and provides continuous, accurate monitoring of oxygen saturation. Table 1 compares our 3D ring oximeter with existing commercial products and academic solutions. The lifetime has been estimated from the datasheets provided by the producers or with the current consumption shown in the previous work and using a 40mAh battery as in our work and 1 acquisition per minute.

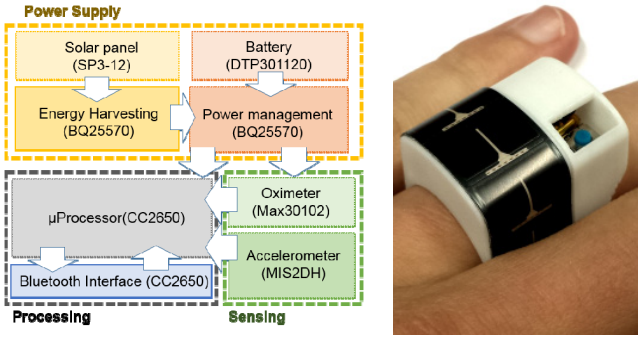

FIGURE 1. Block diagram (left) and image (right) of the proposed smart ring comprising of three main subsystems. 1) Power supply that includes a battery, energy harvesting, and power management. 2) Processing including data acquisition, processing, and wireless interface. 3) Sensing: oximeter and accelerometer.

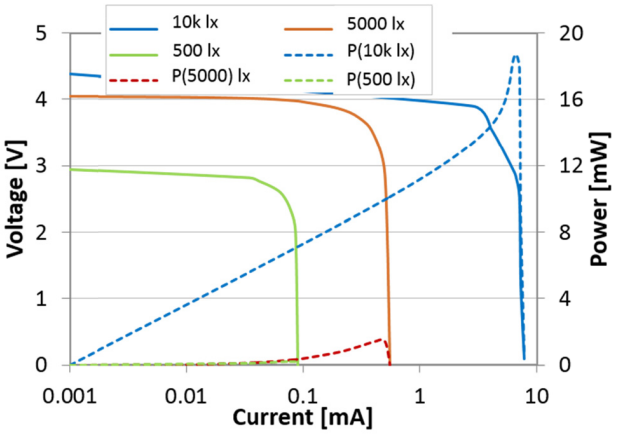

FIGURE 2. The output characteristic of the flat flexible solar panel (SP3-12) at different illumination levels.

The main contributions of the paper are the following:

- Design and implementation of a wireless pulse oximeter into a 3D ring geometry for continuous monitoring of oxygen saturation;
- Implementation of energy harvesting *via* thin and flexible solar panels which are mounted on the 3D case of the ring;
- Onboard processing with an ARM Cortex M3 microcontroller and transmission of only relevant data to minimize the power for the communication;
- In-field test to assess the power consumption and sustainability of the system, as well as its accuracy. The ring oximeter has been benchmarked against standard equipment currently used in the hospitals (Nellcor N-395).

II. SYSTEM ARCHITECTURE

Figure 1 shows the architecture of the smart ring. It consists of a 40mAh Li-Ion battery with a solar energy harvester for power supply, a processing section with BLE connectivity (based on the TI CC2650 [33]) and two sensors, namely an oximeter (MAX30102) and an accelerometer (MIS2DH). As demonstrated in previous works, the accelerometer can be very useful to improve the quality of the measurement when the user is moving [31]. The accelerometer is not exploited in this work, but it will be used in future work. However, it is already present on the current version of the smart ring, and its power already counted in the energy evaluations. The pulse oximeter non-invasively measures the blood oxygenation by shining light at two different wavelengths into the finger and by analyzing the pulsatile component of the reflected intensities [26]. The oximeter sensor controls two LEDs and converts the analog signal from its photodiode into a digital representation for the connected microcontroller. The ring-form of the 3D-printed casing ensures conformal contact with the skin.

A. POWER SUPPLY

The power supply subsystem is designed around the BQ25570 integrated circuit (IC) from Texas Instruments. BQ25570 is the state-of-the-art energy harvester IC, and it is used to recharge the buffering battery with the power harvested by the flexible solar panel which is wrapped around the ring. The IC achieves up to 90% conversion efficiency as it periodically adjusts its internal input-impedance to the Maximum Power Point (MPP) of the panel output characteristic. This parameter changes with the illumination environment. The IC has a double function of charging the batteries using an integrated boost-converter and, simultaneously, of supplying the rest of the system with another integrated high-efficiency buck converter. The supply voltage for the whole system has been chosen to be 1.8V as this voltage minimizes the power and energy consumption of the system, being the lowest voltage supported by the majority of ICs used in the circuit. From a wearable application point of view, the output power, the effective light spectrum, the size, and the flexibility of the cells are of special interest. We selected a flexible panel, Flex Solar Cells SP3-12 [32] that measures only 1cmx5cm and can be laminated on top of the ring. This cell has been characterized to find the available power consumption under different light conditions (expressed in lux [lx]). Fig. 2 shows the measured data for 500 lx (typical for the indoor scenario) 1 klx (typical for cloudy outdoor scenarios) and 10 klx (typical for sunny outdoor scenarios).

The experiments demonstrate that the available power ranges from the maximum power point of 0.18 mW at 500 lx to 18.7 mW at 10 klx, requiring an adaptive harvester circuit. It is worth mentioning the harvested power is reduced to 46.8% when the ring is bent around the ring (10 mm bending radius).

B. PROCESSING AND WIRELESS INTERFACE SUBSYSTEM

This part of the system consists of the Texas Instrument's CC2650 which integrate multiple hardware components (data processing, controlling sensing, communication) in a miniaturized (4mm × 4mm) single chip. The microcontroller has a dual-core architecture with an ARM Cortex M3 for processing, an ARM Cortex M0 core dedicated to the Bluetooth communication and an autonomous sensor controller.

The power-optimized sensor controller runs autonomously, allowing the rest of the processor to stay in standby mode. The direct access to peripherals makes the sensor controller perfectly suited for reading and writing sensor data as well as digital and analog inputs and outputs. The collected sensor data can be efficiently processed at any moment by the Cortex M3 CPU which is waked up by the sensor controller. Its energy efficient sensor controller is another reason why this processor has been selected for this work. The data from the oximeter can be acquired and stored in memory without involving the ARM Cortex M3, improving the energy efficiency of the whole system. The CC2650 also performs low power wireless communications with Bluetooth low energy. The current consumption is only 6.1mA in transmission mode at 0dBm, and 1 μA in standby, resulting in, to our knowledge, the lowest BTLE commercially available.

C. OXIMETER SENSOR AND LOW POWER IMPLEMENTATION OF SpO2 MEASUREMENT

The MAX30102 pulse oximeter, used in our design, has two internal LEDs, namely a red (660nm) and an infrared (880nm) one, and a photo-diode for measuring the reflected light intensity. It provides automatic ambient light cancellation, a 186 byte FIFO register for buffering the sampled data and an I^2C interface for communicating with the CC2650 (using the sensor controller).

The blood oxygen saturation is calculated as follows:

$$SpO_2 = \frac{cHbO_2}{cHbO_2 + cHb} \tag{1}$$

where $cHbO_2$ and cHb are respectively the concentrations of oxygenated and deoxygenated hemoglobin which are calculated from ratios of the photodetector responses during red and IR illumination by using the Modified Lambert-Beer Law. As the interest is in the concentrations of $cHbO_2$ and cHb of the arterial blood, only the pulsatile component of reflected light is considered. A low pass filter eliminates high-frequency noise while the baseline evaluated during the measuring period (4 s) accounts for eventual drift, which is subtracted from the data set. To optimize the power consumption, the active phases of the system were duty-cycled.

During each measurement, the CC2650 processor activates the sensor and reads the signal from the photodetector, so only the sensor controller domain of the microcontroller needs to be enabled, further reducing the power consumption. As soon as all samples are recorded, the more powerful main core, the ARM M3, is activated and processes the data before putting the controller back into standby mode until the next measurement. Independently of the main core, a low power ARM M0 core controls the BLE interface and automatically switches to standby mode when unused. As shown in the next section, this approach reduces the amount of data significantly to be transmitted. Only the processed oxygenation level is communicated, instead of sending all raw data. Moreover, the onboard processing can provide real-time feedback if any anomaly is found in the SpO_2.

III. SENSOR PROCESSING

Hemoglobin molecules in the bloodstream are responsible for transporting oxygen. In the lungs, they load oxygen and release it again at the cells, such that the molecule can be found as unloaded deoxy-hemoglobin (Hb) or oxygen-carrying oxy-hemoglobin (HbO2). The ratio between the concentration of oxygenated hemoglobin and the total concentration of hemoglobin is called oxygen saturation.
Pulse-oximetry

exploits the wavelength-dependent light- absorptions of the oxyhemoglobin and deoxy-hemoglobin molecules. Thus, an oximeter can determine the two hemoglobin concentrations by measuring the light absorption of the blood at two different wavelengths.

Two wavelengths, namely 660nm and 880nm, where the extinction coefficients (absorptivity) of the hemoglobin molecules are separated were used. Carboxyhaemoglobin (COHb) and methemoglobin (MetHb) are other hemoglobin molecules which normally do not have to be considered due to their low concentrations in the blood. Thus the total hemoglobin concentration in the blood sums up to $c_{totalHb}$ and can, therefore, be used to determine the oxygen saturation SpO2 (see Equation 2) [34].

$$\begin{aligned} c_{totalHb} &= c_{HbO_2} + c_{Hb} + c_{COHb} + c_{MetHb} \approx c_{HbO_2} + c_{Hb} \\ SpO_2 &= \frac{c_{HbO_2}}{c_{totalHb}} \approx \frac{c_{HbO_2}}{c_{HbO_2} + c_{Hb}} \end{aligned} \tag{2}$$

To calculate the molecule concentrations for computing the oxygen saturation, the Beer-Lambert law for light absorption in a medium can be used [35]. It puts the light intensity after passing a medium (I) in relation to the incident light intensity (I_0) as shown in equation IV. The attenuation then depends on the absorptivity $\alpha(\lambda)$ of the medium, its concentration c and the length of the optical path l. If the red and infrared light is being shone onto blood, the absorption can be determined with this principle and will mainly depend on the concentration of oxyhaemoglobin and deoxyhemoglobin. These two unknown concentrations cHb and cHbO2 can be directly determined by solving the system of two equations (one for each wavelength), assuming that the path length is known too.

$$\begin{aligned} I &= I_0 \cdot e^{-\alpha(\lambda)\cdot c\cdot l} \\ I_{660nm} &= I_{0,660nm} \cdot e^{-(\alpha_{Hb}(660nm)\cdot c_{Hb} + \alpha_{HbO2}(660nm)\cdot c_{HbO2})\cdot l_{660nm}} \\ I_{880nm} &= I_{0,880nm} \cdot e^{-(\alpha_{Hb}(880nm)\cdot c_{Hb} + \alpha_{HbO2}(880nm)\cdot c_{HbO2})\cdot \log 00nm} \end{aligned} \tag{3}$$

Measuring the intensities on human skin requires data processing because the light passes other layers of tissue and blood vessels, which add to the total absorption of the light. As only the arterial blood wants to be measured, everything except for the pulsating part can just be ignored (constant parts belong to other tissues). All arterial influences are pulsating with the heart rate, making them easily distinguishable from the rest. The input light intensity of the arterial blood is, therefore, the value at the minimum of the pulse, whereas

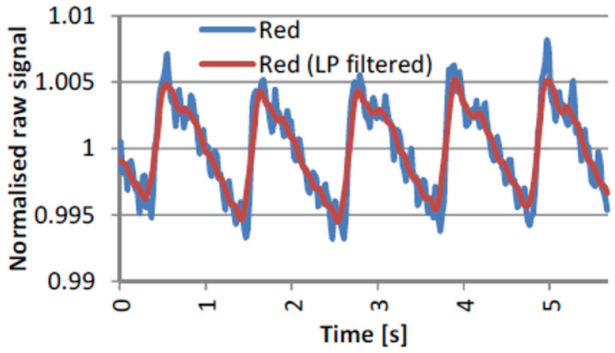

FIGURE 3. Raw oximetry signal when the red light is reflected (blue line in the figure) and its low-pass filtered version (red line). The raw data has been recorded with the smart ring. The pulse rate, as well as the typical notch caused by the flowing-back blood after each heart contraction, can be identified. The ring sampled the sensor at 100Hz.

the output intensity equals the pulsating top of the curve. By taking the logarithm of the intensity-ratio, IV can be solved for cHb and cHbO2. Although the results still contain path-lengths, these factors will cancel out. It must be noted that the path lengths of the different wavelengths are not the same, as the shorter wavelength travels further. Therefore a Differential Pathlength Factor (DPF) has to be multiplied to the affected lengths to account for that. The exact DPF value can be determined through calibration and has been found to show accurate results for a value of 1.4 (on the fingertip).

The MAX30102 oximeter was characterized by testing different sampling rates, LED currents, pulse widths and resolutions to find the setting which consumes the least power while still yielding valuable results. During the tests, a sampling frequency of 100Hz at an averaging setting of 2 with 69 μs pulse width was found to be a good setting for measurements on the finger. The LED current was chosen to be 6.4mA as the best trade-off between power consumption and signal quality.

The raw signal is first processed for removing drift from the signals. Therefore, a high-pass filter was implemented before the actual algorithm. To ensure proper heart-beat recognition for detecting the pulse amplitude, a minimum sampling time off 4 seconds was found to be necessary for averaging the amplitudes over multiple heartbeats. Even with an unusually low heart rate of 30 beats per minute, still, two periods could be averaged for analysis. Sampling inaccuracies were filtered out with a low pass filter, configured with a cut-off frequency below the sampling frequency (see Figure 3).

Our application is not intended to track fast drops of the blood oxygenations as it might be necessary during surgeries, and could, therefore, trade off the measuring period against the power consumption. By choosing a period of once every minute, the power consumption could be reduced by 93.3% (compared to continuous operation). Due to the lack of a floating point unit on the used microcontroller, all divisions and logarithms were carefully converted to fixed point operations by multiplying the operands with constants to decrease the accuracy loss. Experimental results will show that this accuracy of the processing is not affected by this conversion.

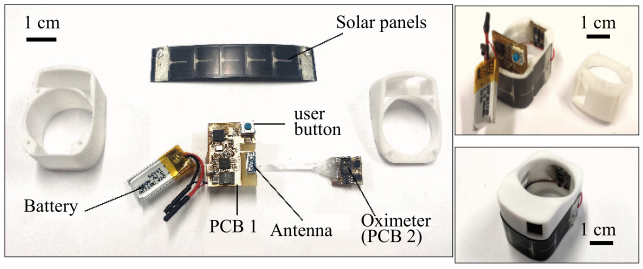

FIGURE 4. Display of the main components of the ring oximeter (left) and its assembly (right top and bottom). The 3D case is 32 mm tall and 22 mm large with an aperture of 10 mm in radius to accommodate the forefinger.

FIGURE 5. Professional Nellcor N-395 pulse oximeter used to compare our solution.

IV. EXPERIMENTAL RESULTS

Accurate and reliable measurements require the sensor to achieve a conformal contact with the skin of the finger to maximize the reflected signal and minimize the movement artifacts. The electronic circuit was split into two separate PCBs connected *via* thin copper wires. The bottom PCB accommodates the optical sensor and an accelerometer that can measure the movements during the measurements and, eventually, correct artifacts. This functionality will be implemented in future works. On the top side, there is more space to accommodate the rest of the components, *i.e.,* energy harvesting, TI-CC2650, interfaces, and the battery. Especially the user button, which is used to activate the measurement procedure manually, and the LEDs, which are used for notification, needed to be placed well-accessible on the top of the device. Fig. 4 shows all the components which form the ring. The two PCBs are connected with a flexible cable and assembled into the case with PCB 1, and PCB 2 mounted on the top and bottom part of the ring, respectively. The flexible solar panel is wrapped around the ring.

A. TEST OF THE OXYGENATION MEASUREMENTS

A professional Nellcor N-395 pulse oximeter served to assess the proper functioning of the ring oximeter (Fig. 5). It features a transmissive sensor clip, which can be attached to the finger during measurement. Like most other professional pulse oximeters, the N-395 has an accuracy of $\pm 2\%$ oxygen saturation in the range of 70% - 100% [36]. Fig. 6 illustrates

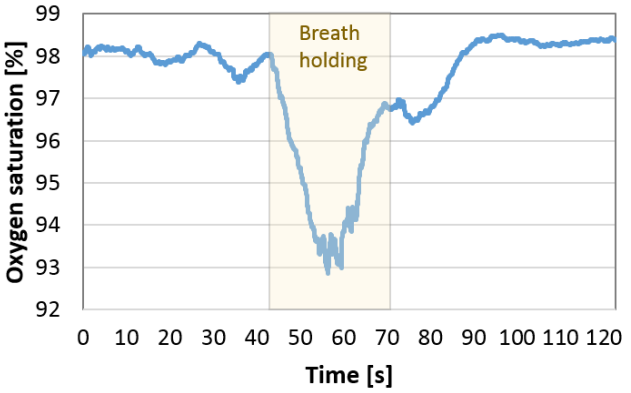

FIGURE 6. Arterial oxygen saturation measurements recorded with the smart ring oximeter during a breath-holding experiment.

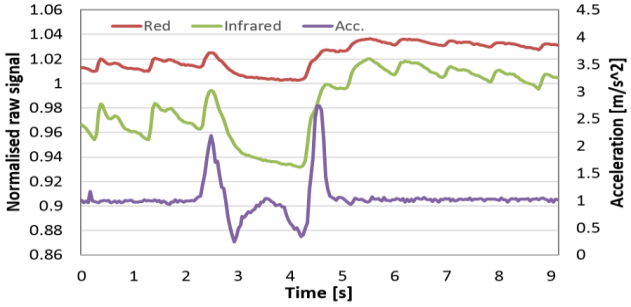

FIGURE 7. Raw oximetry signals (of the reflected red and infrared light) and acceleration data during an experiment where the hand with the worn ring was sequentially raised and lowered twice.

the results of a breath-holding experiment, which is usually performed to mimic occlusions/anomalies in the cardiovascular system.

A typical experiment consists of holding the breath for 30 seconds (marked in light yellow) to cause dropping of 5% of the oxygen saturation. Both the N-395 and the wearable ring registered similar trends and values of the SpO_2. Another experiment consists in measuring the smart ring's raw data in the presence of movement. The signals from the red and infrared LEDs and the onboard accelerator are shown in Fig. 7. As expected, the movements introduce artifacts on the pulse signal. These effects deteriorate the measurement quality of the ring oximeter. It is worth mentioning that, even though this is out of the focus of this work, the sensor-fusion algorithm may compensate for such artifacts.

B. POWER CONSUMPTION MEASUREMENTS AND SELF-SUSTAINABILITY

As presented in Fig. 2, we performed a preliminary solar panel characterization in our lab using different luminosity levels to quantify the harvested energy, also considering the power lost in the conversion. The solar harvesting subsystem, including DC/DC converters and MPPT, has been tested to ensure proper functionality and validate the effective performance.

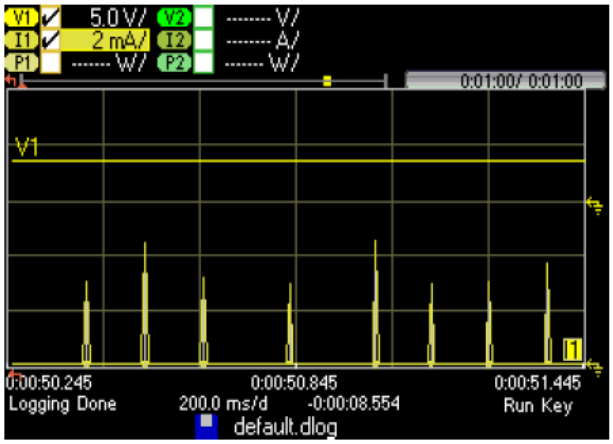

FIGURE 8. Diagram of the system's power consumption during standby mode (measured at the battery).

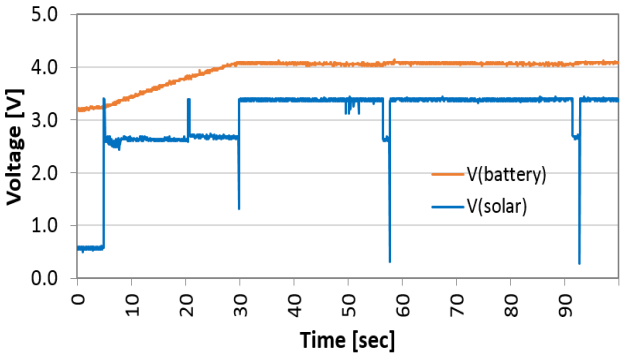

FIGURE 9. Voltage diagram during solar energy harvester testing.

Systematic characterization of the system power consumption for various modes of operation (i.e., idle with BLE on/off, measurement with BLE off/connected) has been performed using the Keysight N6705 power analyzer. Fig. 8 shows an example of a measurement performed in standby mode. The short current pulses (peak values of up to 6mA) are used to periodically inject power into those domains of the processor, which are not switched off during standby mode (timers, sensor controller). This approach avoids static currents and minimizes power consumption.

Fig. 9 shows the voltage during the charging phase of the battery until it reaches the maximum voltage of 4.1V. To adapt the input impedance of the harvester to the solar panel's MPP, the open-circuit voltage (here approximately 3.5V) is tested periodically (peaks during the charging process), making it possible to approximate the MPP.

Additional tests provide information on the input energy from the solar panel (at the MPP) and the efficiency of the harvester. Experiments with 500lx, 1klx, and 10klx illumination reveal the efficiency of our circuit of about 85.2%. Table 2 summarizes the average current and power consumption for the different operation modes.

The implemented application consumes 321.12μW ($P_{measuring}$) on average while conducting one blood

TABLE 2. The power consumption of the ring oximeter measured at the battery.

Mode	Supply Voltage [V]	Average Current Consumption [mA]	Average Power Consumption [mW]
Measuring**Error! Reference source not found.**	3.7	0.086 (0.001 min.) (62.143 max.)	0.312
Processing data	3.7	0.710	2.63
Bluetooth	3.7	2.96	10.98

measurement per minute. Table 2 also shows the minimal and maximum currents during the measurements; the maximum current of 62mA is mainly due to the consumption of the pulse sensor and the activity of the microcontroller to acquire the data. During the processing of the data acquired the microcontroller needs 2.63mW of power, while the time to process the data (t_{proc}) is around 0.100ms. During data transmission with BLE connected, the power consumption measured reaches 10.98mW (P_{BLE}). In the case of the transmission of all raw data acquired by the sensor, the transmission time would amount to 128s per hour. To improve the energy efficiency of the communication, it is possible to send only the processed data of the SpO_2 (2-bytes per acquisition). In this case, the time to send the data is reduced to 0.160 seconds. To determine the lifetime of the device, the hourly communication sequences have to be included in the calculation of the daily energy consumption using Equation 4.

$$E_{daily} = t_{measuring} * P_{measuring} + t_{BLE} * P_{BLE} \tag{4}$$

where $t_{measuring}$ is the time spent during the measurement and t_{BLE} is the time to transmit data via Bluetooth. The calculation below provides an example when all raw data are transmitted:

$$\left(86400\frac{s}{day} - 128\frac{s}{h} * 24\frac{h}{day}\right) * 321.12\mu W + \left(128\frac{s}{h} * 24\frac{h}{day}\right) * 10.98mW = 60.488J \tag{5}$$

On the other hand in case the data are processed on-board and then sent equation 4 needs to take in count also the power and the time to process the data. Equation 4 can then updated as:

$$\begin{aligned} E_{daily} &= t_{measuring} * P_{measuring} + t_{proc} * P_{proc} + t_{BLE} * P_{BLE} \\ &\times \left(86400\frac{s}{day} - 0.16\frac{s}{h} * 24\frac{h}{day}\right) * 321.12\mu W \\ &+ \left(0.1\frac{s}{h} * 24\frac{h}{day}\right) * 2.63mW + \left(0.16\frac{s}{h} * 24\frac{h}{day}\right) \\ &* 10.98mW = 27.792J \end{aligned} \tag{6}$$

where t_{proc} is the time needed to process the data to exact and P_{proc} the power consumption of the MCU processing the data. Using equation 6, the daily energy consumption in case of onboard processing is only 27.7J per day instead of 60.5J resulted by equation 5. This results to be 53% less energy than the version transmitting raw data, which demonstrates the energy efficiency of the onboard data processing of our proposed solution.

TABLE 3. Application scenario to achieve self-sustainability.

Scenario	Time outdoor (>10klux)	Time office lamp (5klux)	Time indoor (500lux)	Battery Energy balance $=E_{harvested}/E_{consumed}$ $=E_{input}*\eta_{harv}/E_{consumed}$
	Pin=18.56mW	Pin=1.44mW	Pin=0.18mW	
	Peff=7.4mW	Peff=0.57mW	Peff=0.07mW	
8h outside	8h	0	4h	759%
4h outside	4h	0	8h	385%
1h outside	1h	0	11h	104%
Office day	0	8h	4h	62%
Only lunch outside	0.5h	8h	3.5h	109%
At home	0	0	12h	11%

The solar energy harvester needs to compensate for the energy loss in the battery on a daily basis o achieve self-sustainable operation. To have a worst case scenario and to show the low power of our solution, we used the daily energy in the case of raw data. The characterization of the solar panel showed that during direct sunlight illumination an input power of 18.56mW is supplied to the harvester circuit (Fig. 2). Considering the reduced efficiency (46.8%) due to the bending of the panels around the ring and the efficiency of the voltage converter (85.2%) self-sustainability is achieved with about 63.5 minutes of sunlight exposure (at 1 klx). Equation 7 reported below provides the details on the calculation:

$$\begin{aligned} t_{min} &= \frac{E_{exp,d}}{P_{eff} * \eta_{harv}} = \frac{28.225Ws}{(18.56mW * 0.468) * 0.852} \\ &= 3814s \approx 63.5minutes \end{aligned} \tag{7}$$

As the battery allows for buffering of energy for multiple days, other charging options are possible. This means that exposing the device for multiple hours to sunlight would allow the battery to store energy for operating multiple days (up to 18 days with less or no sunlight). Table 3 presents a few scenarios, which are based on the measurements of the energy input and consumption. Both the reduction of input power due to the effective area (46.8%) and the harvesting efficiency (85.2%) have been included in these calculations.

The low solar power in the office requires having lunch outdoors for half an hour to compensate for all daily energy expenses. On the other hand, hiking 4h outdoors would compensate for almost three extra days.

V. CONCLUSION

We presented a wearable smart ring, which can provide accurate and long-term information about blood oxygen saturation. Duty-cycling of sensor activities in combination with

onboard processing and solar energy harvesting, ensure self-sustainability, which was demonstrated in realistic scenarios. By measuring the blood oxygenation once every minute with a sampling rate of 100 samples/s, accurate results were achieved with a daily energy consumption of only 28 Joule, including hourly BLE transmissions of processed measurement results. This allows the system to be self-sustainable with just 64 minutes of sunlight per day or 12h of indoor home light. The smart ring oximeter, demonstrated here, is just one example of possible self-sustainable applications and the hardware/software design can be extended to other sensors to achieve wearable self-powered multimodal sensing. Future works will focus on improving the accuracy of the system even in the presence of artifacts, exploiting the accelerometer that is already present on the smart ring.

REFERENCES

[1] Y. Khan, A. E. Ostfeld, C. M. Lochner, A. Pierre, and A. C. Arias, "Monitoring of vital signs with flexible and wearable medical devices," *Adv. Mater.*, vol. 28, no. 22, pp. 4373–4395, 2015.

[2] M. Magno, C. Spagnol, L. Benini, and E. Popovici, "A low power wireless node for contact and contactless heart monitoring," *Microelectron. J.*, vol. 45, no. 12, pp. 1656–1664, 2014.

[3] M. Magno, L. Benini, C. Spagnol, and E. Popovici, "Wearable low power dry surface wireless sensor node for healthcare monitoring application," in *Proc. IEEE 9th Int. Conf. Wireless Mobile Comput., Netw. Commun. (WiMob)*, Oct. 2013, pp. 189–195.

[4] L.-B. Chen, H.-Y. Li, W.-J. Chang, J.-J. Tang, and K. S.-M. Li, "WristEye: Wrist-wearable devices and a system for supporting elderly computer learners," *IEEE Access*, vol. 4, pp. 1454–1463, 2016.

[5] J. LaPier and M. Chatellier, "Optimizing portable pulse oximeter measurement accuracy and consistency during exercise," *J. Acute Care Phys. Therapy*, vol. 8, no. 3, pp. 96–105, 2017.

[6] A. H. Sapci and H. A. Sapci, "The effectiveness of hands-on health informatics skills exercises in the multidisciplinary smart home healthcare and health informatics training laboratories," *Appl. Clin. Inf.*, vol. 8, no. 4, pp. 1184–1196, 2017.

[7] P. J. Soh, G. A. E. Vandenbosch, M. Mercuri, and D. M. M.-P. Schreurs, "Wearable wireless health monitoring: Current developments, challenges, and future trends," *IEEE Microw. Mag.*, vol. 16, no. 4, pp. 55–70, May 2015.

[8] G. Fortino, S. Galzarano, R. Gravina, and W. Li, "A framework for collaborative computing and multi-sensor data fusion in body sensor networks," *Inf. Fusion*, vol. 22, pp. 50–70, Mar. 2015.

[9] S. Qiu, Z. Wang, H. Zhao, L. Liu, and Y. Jiang, "Using body-worn sensors for preliminary rehabilitation assessment in stroke victims with gait impairment," *IEEE Access*, vol. 6, pp. 31249–31258, 2018.

[10] K. D. McClatchey, Ed. *Clinical Laboratory Medicine*. Philadelphia, PA, USA: Lippincott Williams & Wilkins, 2002.

[11] V. Andrianopoulos, B. R. Celli, F. M. E. Franssen, V. M. Pinto-Plata, P. M. A. Calverley, L. E. G. W. Vanfleteren, I. Vogiatzis, J. Vestbo, A. Agusti, P. S. Bakke, S. I. Rennard, W. MacNee, R. Tal-Singer, J. C. Yates, E. F. M. Wouters, and M. A. Spruit, "Determinants of exercise-induced oxygen desaturation including pulmonary emphysema in COPD: Results from the ECLIPSE study," *Respiratory Med.*, vol. 119, pp. 87–95, Oct. 2016.

[12] L. A. Clifton, D. A. Clifton, M. A. F. Pimentel, P. J. Watkinson, and L. Tarassenko, "Predictive monitoring of mobile patients by combining clinical observations with data from wearable sensors," *IEEE J. Biomed. Health Inform.*, vol. 18, no. 3, pp. 722–730, May 2014.

[13] U. Ha, Y. Lee, H. Kim, T. Roh, J. Bae, C. Kim, and H.-J. Yoo, "A wearable EEG-HEG-HRV multimodal system with simultaneous monitoring of tES for mental health management," *IEEE Trans. Biomed. Circuits Syst.*, vol. 9, no. 6, pp. 758–766, Dec. 2015.

[14] M. Magno, M. Pritz, P. Mayer, and L. Benini, "DeepEmote: Towards multi-layer neural networks in a low power wearable multi-sensors bracelet," in *Proc. 7th IEEE Int. Workshop Adv. Sensors Interfaces (IWASI)*, Jun. 2017, pp. 32–37.

[15] G. Fortino, R. Giannantonio, R. Gravina, P. Kuryloski, and R. Jafari, "Enabling effective programming and flexible management of efficient body sensor network applications," *IEEE Trans. Hum.-Mach. Syst.*, vol. 43, no. 1, pp. 115–133, Jan. 2013.

[16] M. A. Suster, N. H. Vitale, D. Maji, and P. Mohseni, "A circuit model of human whole blood in a microfluidic dielectric sensor," *IEEE Trans. Circuits Syst. II, Exp. Briefs*, vol. 63, no. 12, pp. 1156–1160, Dec. 2016.

[17] T. N. Le, M. Magno, A. Pegatoquet, O. Berder, O. Sentieys, and E. Popovici, "Ultra low power asynchronous MAC protocol using wake-up radio for energy neutral WSN," in *Proc. 1st Int. Workshop Energy Neutral Sens. Syst.*, 2013, p. 10.

[18] M. Magno, L. Benini, L. Gaggero, J. P. La Torre Aro, and E. Popovici, "A versatile biomedical wireless sensor node with novel drysurface sensors and energy efficient power management," in *Proc. 5th IEEE Int. Workshop Adv. Sensors Interfaces (IWASI)*, Jun. 2013, pp. 217–222.

[19] F. Wu, J.-M. Redouté, and M. R. Yuce, "WE-safe: A self-powered wearable IoT sensor network for safety applications based on LoRa," *IEEE Access*, vol. 6, pp. 40846–40853, 2018.

[20] L. Zuo, S. K. Islam, I. Mahbub, and F. Quaiyum, "A low-power 1-V potentiostat for glucose sensors," *IEEE Trans. Circuits Syst., II, Exp. Briefs*, vol. 62, no. 2, pp. 204–208, Feb. 2015.

[21] Y.-J. Kim, H. S. Bhamra, J. Joseph, and P. P. Irazoqui, "An ultra-low-power RF energy-harvesting transceiver for multiple-node sensor application," *IEEE Trans. Circuits Syst. II, Exp. Briefs*, vol. 62, no. 11, pp. 1028–1032, Nov. 2015.

[22] M. Magno, L. Spadaro, J. Singh, and L. Benini, "Kinetic energy harvesting: Toward autonomous wearable sensing for Internet of Things," in *Proc. Int. Symp. Power Electron., Elect. Drives, Automat. Motion (SPEEDAM)*, Jun. 2016, pp. 248–254.

[23] M. Magno and D. Boyle, "Wearable energy harvesting: From body to battery," in *Proc. 12th Int. Conf. Design Technol. Integr. Syst. Nanoscale Era (DTIS)*, Apr. 2017, pp. 1–6.

[24] T. Wu, F. Wu, J.-M. Redouté, and M. R. Yuce, "An autonomous wireless body area network implementation towards IoT connected healthcare applications," *IEEE Access*, vol. 5, pp. 11413–11422, 2017.

[25] G. Pang and C. Ma, "A neo-reflective wrist pulse oximeter," *IEEE Access* vol. 2, pp. 1562–1567, 2014.

[26] P. Singh, G. Kaur, and D. Kaur, "Infant monitoring system using wearable sensors based on blood oxygen saturation: A review," in *Proc. Int. Conf. Intell., Secure, Dependable Syst. Distrib. Cloud Environ.* Cham, Switzerland: Springer, 2017, pp. 162–168.

[27] C. Hebbale and K. Fu, "Wearable on-demand oxygen therapy," in *Proc. Int. Design Eng. Tech. Conf. Comput. Inf. Eng. Conf.*, Aug. 2016, Art. no. V003T11A009.

[28] J. Kim, P. Gutruf, A. M. Chiarelli, S. Y. Heo, K. Cho, Z. Xie, A. Banks, S. Han, K.-I. Jang, J. W. Lee, K.-T. Lee, X. Feng, Y. Huang, M. Fabiani, G. Gratton, U. Paik, and J. A. Rogers, "Miniaturized battery-free wireless systems for wearable pulse oximetry," *Adv. Funct. Mater.*, vol. 27, no. 1, 2017, Art. no. 1604373.

[29] Y. Fu and J. Liu, "System design for wearable blood oxygen saturation and pulse measurement device," in *Proc. 6th Int. Conf. Appl. Hum. Factors Ergonom. (AHFE)*, vol. 3, 2015, pp. 1187–1194.

[30] G. Ma, W. Zhu, J. Zhong, T. Tong, J. Zhang, and L. Wang, "Wearable ear blood oxygen saturation and pulse measurement system based on PPG," in *Proc. IEEE SmartWorld, Ubiquitous Intell. Comput., Adv. Trusted Comput., Scalable Comput. Commun., Cloud Big Data Comput., Internet People Smart City Innov. (SmartWorld/SCALCOM/UIC/ATC/CBDCom/IOP/SCI)*, Oct. 2018, pp. 111–116.

[31] P. J. Chacon, L. Pu, T. H. da Costa, Y.-H. Shin, T. Ghomian, H. Shamkhalichenar, H.-C. Wu, B. A. Irving, and J.-W. Choi, "A wearable pulse oximeter with wireless communication and motion artifact tailoring for continuous use," *IEEE Trans. Biomed. Eng.*, vol. 66, no. 6, pp. 1505–1513, Jun. 2019.

[32] FlexSolarCells. *SP3-12*. Accessed: Sep. 3, 2018. [Online]. Available: http://www.flexsolarcells.com/indexfiles/OEMComponents/FlexCells/specificationsheets/00FlexSolarCells.comPowerFilmSolarSP3-12SpecificationSheet.pdf

[33] Texas Instruments. *CC2650 SimpleLink Multistandard Wireless MCU*. Accessed: Sep. 3, 2018. [Online]. Available: http://www.ti.com/lit/ds/symlink/cc2650.pdf

[34] S. Hayomond, "Oxygen saturation: A guide to laboratory assessment," Clin. Lab. News, Washington, DC, USA, Tech. Rep., 2006.

[35] R. R. Kroll, J. G. Boyd, and D. M. Maslove, "Accuracy of a wrist-worn wearable device for monitoring heart rates in hospital inpatients: A prospective observational study," *J. Med. Internet Res.*, vol. 18, no. 9, 2016, Art. no. e253.
[36] *Operator's Manual N-395 Pulse Oximeter*, Mallinckrodt, Bedminster, NJ, USA, 2000.

MICHELE MAGNO (SM'13) received the master's and Ph.D. degrees in electronic engineering from the University of Bologna, Bologna, Italy, in 2004 and 2010, respectively, where he is currently a Research Fellow. He is also a Postdoctoral Researcher with ETH Zürich, Zürich, Switzerland. He has authored over 100 papers in international journals and conferences. His current research interests include wireless sensor networks, wearable devices, energy harvesting, low power management techniques, and extension of the lifetime of batteries-operating devices.

GIOVANNI A. SALVATORE received the bachelor's degree in electronics and the master's degree in micro and nanotechnology from the Polytechnic University of Turin, in 2004 and 2006, respectively, and the Ph.D. degree from EPFL, in 2011, for the research on ferroelectric transistors (EPFL thesis 4990). He is a Scientist with the ABB Corporate Research Center. He has received the 2006 Accenture Award from the Polytechnic University of Turin as the best thesis in electronics for his work on a new nanoimprinting technique developed in the RLE at MIT. His doctoral dissertation has received the 2012 ABB Award.

PETAR JOKIC received the M.Sc. degree in electrical engineering and information technology from ETH Zürich, Zürich, Switzerland, in 2016. He is currently pursuing the Ph.D. degree with CSEM SA, Zürich, Switzerland, in collaboration with the Integrated Systems Laboratory, ETH Zürich. His main research interests include low-power embedded systems, machine learning, computer vision, and smart sensing.

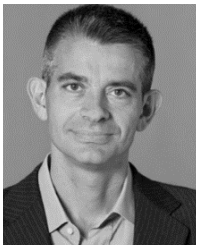

LUCA BENINI (F'07) has served as the Chief Architect for the Platform 2012/STHORM Project with STMicroelectronics, Grenoble, France. He has held visiting and consulting researcher positions at EPFL, Lausanne, Switzerland, IMEC, Leuven, Belgium, Hewlett-Packard Laboratories, Palo Alto, CA, USA, and Stanford University, Stanford, CA, USA. He is currently the Chair of digital circuits and systems with ETH Zürich, Zürich, Switzerland, and a Full Professor with the University of Bologna, Bologna, Italy. He is also active in the areas of energy-efficient smart sensors and sensor networks for biomedical and ambient intelligence applications. He has authored over 700 papers in peer-reviewed international journals and conferences, four books, and several book chapters. His current research interests include energy-efficient system design and multicore SoC design. He is a Fellow of the ACM and a member of the Academia Europaea.